RSC Publishing Faraday Discussions

FD175:Studies of the Dynamics of Biological Macromolecules with Au Nanoparticle-DNA Artificial Molecules

Journal:	*Faraday Discussions*
Manuscript ID:	FD-ART-07-2014-000149.R1
Article Type:	Paper
Date Submitted by the Author:	29-Jul-2014

Complete List of Authors:	Chen, Qian; University of California, Berkeley, Department of Chemistry; Miller Institute for Basic Research in Science, Smith, Jessica; University of California, Berkeley, Department of Chemistry Rasool, Haider; University of California, Berkeley, Department of Physics Alivisatos, Paul; University of California, Berkeley, Chemistry Zettl, Alex; University of California at Berkeley, Department of Physics

Studies of the Dynamics of Biological Macromolecules with Au Nanoparticle-DNA Artificial Molecules

Qian Chen[1,2,3], Jessica M. Smith[1,2], Haider I. Rasool[2,4], Alex Zettl[2,4], A. Paul Alivisatos[1,2,*]

Abstract

The recent development of graphene liquid cell, a nanoscale version of liquid bubble wrap, is a breakthrough for in situ liquid phase electron microscopy. Using ultrathin graphene sheets as the liquid sample container, graphene liquid cells have allowed the unprecedented atomic resolution observation of solution phase growth and dynamics of nanocrystals. Here we explore the potentials of this technique to probe nanoscale structure and dynamics of biomolecules in situ, using artificial Au nanoparticle-DNA artificial molecules as model systems. The interactions of electrons with both the artificial molecules and the liquid environment have been demonstrated and discussed, to reveal both the opportunities and challenges of using graphene liquid cell EM as a new method of bio-imaging.

Introduction

It has been a challenging goal in microscopy to visualize, and potentially modulate, the transformative kinetics of biomolecules during biological reactions at the nanometer resolution in their native liquid environment.[1-13] Such dynamics involving morphological details are critical to the functions of individual biological molecules, the feedback network of biological processes, and biomedical applications. For example, the folding and unfolding of proteins have inspired extensive theoretical and simulation efforts,[2] to understand the molecular mechanisms of the exposing and hiding of active sites or binding pockets. In contrast, experimental efforts that can probe the conformational dynamics of biomolecules are largely limited due to the lack of an imaging tool that can resolve *in-situ* dynamics at the nanoscale.

The previous focus in the development of experimental approaches has been on two strategies, both of which have great success as well as limitations: pushing the spatial resolution for dynamic imaging techniques such as super-resolution optical microscopy,[5,14,15] and pushing the dynamic capability for high spatial resolution techniques such as cryo electron microscopy[1] and x-ray crystallography[3,4]. Super-resolution optical microscopy, in its various forms, can have the record spatial resolution of ~15 nm, achieved usually from fitting of the point spread function of the emission of individual fluorescent labels. This mechanism of imaging already has its own limitation: morphology of biomolecules can only be generated when the whole biomolecule is covered with labeling agents, which is not experimentally easy and also poses complications in possible interference effects from labeling agents. On the other hand, cryo electron microscopy has developed a suite of imaging and analysis techniques that can generate the three-dimensional (3D) shape of biomolecules at sub nm resolution. But TEM was considered as incompatible with the existence of a liquid sample and thus dynamics in liquid due to its high vacuum working

condition. So in cryo EM technique, the biological samples are embedded in vitrified ice, leaving only snapshots of the conformational states of biomolecules along their dynamic trajectory during reactions. X-ray crystallography shares similar limitations with the additional constraint that it can work only on the crystalline forms of biomolecules. This constraint is more pronounced when the relevant functional states of the biomolecules are not necessarily their bulk crystalline forms. For example, membrane proteins are still presented as a great challenge for x-ray crystallography since they function and transform in close proximity with the cellular membrane.

Here we investigate the opportunities and challenges of a third strategy towards the elusive nanoscale dynamics in biological systems: graphene liquid cell TEM, with the unique advantage of retaining a native liquid environment, and the capability of capturing continuous dynamics at nanometer resolution.[13,16] In principle, graphene liquid cell TEM integrates the powers of the previous two approaches and can thus probe a large sample space that is not approachable before in bio-imaging. It allows samples to be in a liquid environment, like super-resolution optical microscopy, but now can see biomolecular morphological details. It has ultrahigh spatial resolution, just like cryo EM and x-ray crystallography, but now the samples are in their native liquid environment. In comparison to the conventional thick-walled liquid phase EM strategies using Si_3N_4 to hold liquid against high vacuum,[17-21] graphene liquid cells wrap liquid samples using two graphene layers and seal the sample via the van der Waals force between two graphene layers. In this liquid cell configuration, we can minimize the loss of imaging electrons from the one-atom thick graphene window. The atomic resolution imaging capability of EM can be thus maintained despite the liquid molecules surrounding the sample, which is potentially crucial for the observation of low atomic numberbiological samples in liquid. The van der Waals sealing between graphene layers can also minimize the possible contaminations resulting from adhesive spacers.

Meanwhile, the traditionally identified complication with high spatial resolution imaging techniques can persist here: the probing beams, electron beam or x-ray, have high energy that interacts with, and sometimes damage, the sample being imaged. This complication is an important aspect of concern for the broad use of liquid phase EM in imaging nanoscale dynamics of biomolecules. Still graphene has its own unique properties that make it more advantageous than other window materials for liquid phase EM. Our earlier work,[13] as well as other recent independent research,[9,22,23] has observed graphene can help increase the electron beam tolerance of samples, such as an inorganic MoS_2 lattice, and ferritin molecules by wrapping the samples inside. While detailed mechanisms are still under investigation, the speculation is that graphene's ability to rapidly conduct heat and charges can play a role.

The model system we chose to image here is 3D shaped Au-DNA artificial molecules, to study and quantify the effect of electron beam on the DNA molecules during the imaging process.

Such artificial molecules can demonstrate: 1) the effect of electron beam on DNA molecules, detected from the easily visible motions of Au nanoparticles; 2) the determination of 3D shape and dynamics of biomolecules that can be generalized to other small and low-contrast biomolecules. In addition, Au nanoparticles inside the artificial molecules have plasmonic coupling that is sensitive to the construction of the artificial molecules. They have been extensively used as "plasmon rulers"[24-26] to detect the dynamics and activity of biomolecules, but with their real 3D configuration in solution not easily probed. Imaging these artificial molecules in their working liquid environment is also crucial for their design towards optimized optical property for bio-sensing.

Experimental Procedures

Gold Nanoparticle Preparation: Citrate-stabilized 5 nm gold nanoparticles (NPs) (83 nM) were purchased from Ted-Pella, Inc. (Redding, CA). We first stirred such NP solutions with an excess (1 mg BSPP/1mL deionized water) of bis(p-sulfanatophenyl)phenyl-phosphine (BSPP from Strem Chemicals, Inc., Newburyport, MA) overnight. Later, we collected the NPs, now coated with BSPP by centrifuging the solution at 3000 rpm for 15 mins. We then removed the supernatant solution and resuspended the NPs in BSPP solution (1 mg BSPP/1mL deionized water). Our stock solution was concentrated to 2 μM, and was kept at ambient temperature when not in use.

Preparation of single-stranded (ss) DNA: We obtained our ssDNA of desired lengths from Integrated DNA Technologies Inc. (Coralville, IA). The 5' ends were modified with hexylthiol disulfide linkers, and then ssDNA were resuspended in 10 mM Tris buffer containing 0.5mM EDTA in a ~100 μM concentration.

Preparation of Au-ssDNA conjugates: In one reaction, we mixed 70 μL stock solution of Au NPs, 1.5 μL ssDNA stock solution, 10 μL BSPP (5 mg/mL in deionized water), with 10 μL 500 mM NaCl solution, and had them react overnight without stirring at room temperature. The reaction mixture was then mixed with 10 μL of 20 mM poly(ethylene glycol) methyl ether thiol (MPEG) and reacted for 2 hours to replace the BSPP ligands on the Au NPs. The solution then went through high performance liquid chromatography (HPLC) to collect Au NPs with one and two ssDNA on the surface separately, depending on the desired nanoconjugate structure.

Preparation of trimers and pyramids: For trimers, Au nanoparticles conjugated with two ssDNA were mixed and hybridized with Au-ssDNA monoconjugates twice in amount at room temperature overnight. Then reacted solution went through an Agarose gel (3 wt% in deionized water) in electrophoresis to obtain Au-ds DNA conjugates, trimers, from unreacted Au-ss DNA monoconjugate. The electrophoresis was done in 0.5 x tris-borate-EDTA (TBE) buffer. The gels were run for 1 hour at 125 V, after which several distinct bands were visible. We extracted

dimers, or trimers, by cutting the gel at the end of the proper band and immersing the gel piece in 0.5 x TBE buffer and 200 mM NaCl solution. The obtained Au-dsDNA nanoconjugate solution was stocked in fridge when not in use. For pyramids, we followed the procedure in reference 25, but used the DNA strands design such that one edge of the pyramids is shorter than the others.

Preparation of graphene covered TEM grids: The base TEM grids are Quantifoil R1.2/1.3 300 Mesh Au holey carbon TEM grids purchased from SPI supplies. These TEM grids were pressed against graphene grown on Cu foil via chemical vapor deposition. A drop of isopropanol was cast on the Cu foil to immerse the pressed TEM grids to bind them with graphene as isopropanol evaporates. Then the Cu foil together with attached TEM grids up towards the air were put on the surface of a sodium persulfate (Sigma Aldrich) solution (10 mg/ mL) which etched away the Cu foil, leaving TEM grids coated with graphene. Such TEM grids were subsequently rinsed with deionized water three times to wash off the etching solution, and were left dry for further use.

Loading liquid sample into graphene liquid cell: We laid one graphene coated TEM grid onto a hard substrate such as a glassslide with the graphene side facing upwards. One tiny droplet (diameter ¼~1/3 of the TEM grid diameter) of the aqueous solution was deposited onto the center of the TEM grid. Then the other graphene coated TEM grid was put from above to cover the bottom TEM grid and the droplet. During the slight evaporation of water after 10 mins in the air, the top and bottom TEM grids were brought into close contact and kept the rest of the solution intact and sealed.

Microscopy: The TEM imaging was performed on LaB6 Tecnai G2 S-TWIN TEM at 200 kV. An accelerating voltage of 200 kV was used to obtain enough contrast and also to balance between avoiding damaging graphene layer and lowering radiation damage. We set 0.1 seconds of exposure time, 0.9 seconds of read out time, and therefore 1 seconds of entire frame time to acquire time-serial images.

Results

Graphene liquid cell imaging of 3D pyramidal artificial molecules

EM imaging of 3D structure and dynamics of biomolecules has two prerequisites: first, to be able to visualize low contrast, or sometimes invisible, biomolecules with morphology details under EM, and second, to be able to obtain the 3D structure of biomolecules from their 2D projections. Cryo EM developed staining methods using heavy metal ions to enhance the contrast and thus the visibility of biomolecules under EM. In addition, cryo EM relies on the homogeneity of biomolecules at a particular functional state, to reconstruct the 3D structure of biomolecules from snapshots of millions of randomly oriented biomolecules. Using 3D shaped artificial molecules, we demonstrated our proposed strategies towards solving these two issues. The biomolecules,

double stranded DNA (dsDNA), in the artificial molecules are too thin to be seen directly under TEM, and we show how the decoration of a specific staining agent, tiny Au nanoparticles, can help capture the status of dsDNA and enable us to detect its conformational change. As to the 3D structure, instead of generating one structure from millions of molecules, we are able to obtain a series of 2D projections of one particular artificial molecule and to construct the 3D model accordingly.

Our 3D model artificial molecule is of pyramidal shape, with four Au nanoparticles positioned at the vertices and six dsDNA as the bridges. These pyramids are of the simplest geometric shape that extends into 3 dimensions, enabling multiplexed probing of distance or reaction dynamics along different directions. Moreover, the pyramidal arrangement mimics the atomic backbone of glyceraldehyde, the smallest commonly used chiral molecule. Theoretical calculations have predicted such pyramidal artificial molecules, once their symmetry is broken, can generate circular dichroism signals in addition to the geometry-dependent back scatterings from coupled plasmons. Many experimental strategies were suggested to introduce such chirality in pyramids[25], including using Au nanoparticles of different sizes, or different double stranded DNA determined edge lengths. To bring in the practical use of these artificial molecules beyond their use as model systems, we designed their DNA linker sequence such that the tetrahedral DNA constructs, if assembled and base-paired successfully, have one bond shorter than the others (see the red line in **Figure 1**). This strategy, if successful, can serve as the first step towards more variations in DNA linker lengths that eventually generates chirality in structure.

Conventional dry TEM imaging of the final assembled artificial molecules can show whether the Au nanoparticles are in proximity, but cannot resolve their 3D arrangement in their native liquid environment, crucial to their optical properties and applications as biosensors. Backbone structure of the artificial molecules can be distorted during dry TEM sample preparation due to strong capillary force from the meniscus of evaporating solvent. As shown in **Figure 2**, the component Au nanocrystals of a dimeric molecule were dragged altogether into a spacing of ~5 nm despite the expected 15 nm double stranded DNA linker in between. Note that previous studies using small angle x-ray scattering[26] clearly demonstrated that in the solution phase the bond length of the same model dimeric molecules closely follows their linker length. So it is speculated the capillary force can overwhelm the rigid linker and collapse their otherwise well-defined geometric configuration. Likewise, 3D artificial molecules get flattened onto the TEM grid, leaving hardly any information for their 3D configuration (see **Figure 2**). This loss of 3D information poises to be a great challenge since small angle x-ray, the alternative technique to probe the bond length between component artificial atoms, has difficulty interpreting 3D conformation data, not to mention that small angle x-ray can probe only the ensemble interparticle distances.

Using graphene liquid cell EM, we reconstructed the 3D configuration of pyramidal shaped artificial molecules in their native liquid environment. We sandwiched the solution of pyramids

between two graphene layers and captured their dynamics under TEM. The Au nanoparticles we used are small, around 5 nm in diameter, in order to minimize their effect on biomolecules as the "staining" agent. These small Au nanoparticles can easily be seen under TEM, in comparison with the lower spatial resolution obtained from thick-walled Si_3N_4 liquid chamber. We see this advantage of graphene liquid cell EM as crucial for the imaging of low-contrast biomolecules as well as biomolecules stained with small high contrast agents. Here we watched one pyramid tumbling, due to the surrounding liquid environment, and recorded its continuous rotations as a TEM movie. Every snapshot in the movie has one 2D projection of the pyramid, and one set of six measurable projected distances between the four component Au nanoparticles. This is our raw data that can be obtained independently for every snapshot. Then we employ the iterative optimization method described in detail in an earlier report in this laboratory.[13] In short, we assume three bond lengths as the inputs (see l_1, l_2, l_3 in **Figure 1**), and calculate the 3D coordinates of particles B, C, D relative to particle A based upon the inputs and measured projected distances. Now that we have the 3D configuration of the pyramids, we further calculated the other unknown bond lengths (see l_4, l_5, l_6 in **Figure 1**). We did the same calculation for each frame in a continuous movie, and optimized the three inputs until the variances of the three calculated bond lengths reach their minimums, which means the 3D configurations obtained from all the snapshots can converge into one structure.

Several observations can be concluded from this remodeling. The calculated bond lengths are consistent with our DNA design. As shown in the graph of **Figure 1** and representative TEM and 3D configurations shown in **Figure 3**, one bond is indeed distinctly shorter than the other two bonds. And the two longer bonds are not only comparable with each other in length, but also comparable with the three input lengths. This consistency demonstrates that our solution-phase based DNA directed assembly into artificial molecules was able to introduce bond length difference into pyramidal shapes. More work is currently in progress to design DNA sequence that can base pair into chiral pyramids for their unique optical properties. More importantly, this convergence into one 3D configuration of pyramid indicates the geometric configuration of the pyramid stays intact during this time window of imaging. Otherwise, the pyramids will be distorted to different extent and to different shapes during the imaging process. This unique feature indicates the compatibility of graphene liquid cell TEM with imaging of other samples involving biomolecules, and eventually, even biomolecules themselves. The principle of imaging 3D shapes of biomolecules, although demonstrated here in the manner of "coarse-grained" staining, is demonstrated in this example, and can be generalized to other biomolecules.

The electron beam effect

Interaction with the artificial molecules:

Now that we have shown how a projected image relates to the 3D configuration of the pyramids, we can visualize the structural damage of pyramids induced by electron beam in real time. For the TEM imaging of biomolecules, electron beam has been found to induce dramatic structure changes through ionization and consequently bond breakage and bond rearrangements. Extensive studies have been done for biomolecules at cryogenic temperatures, showing that radiation damage is reduced significantly when biomolecules are embedded in a layer of vitrified ice, with the limitation that the samples are also locked in place and become stationary.

Recent EM imaging of liquid phase sample started to suggest new mechanisms of lowering such radiation damage, and allowing imaging of biomolecules at higher spatial resolution and for longer observation time. Reports using Si_3N_4 liquid cell EM techniques[6,8,10,12] argued that the native liquid environment attenuates the structural distortion of bio-samples, including both proteins and living cells, significantly under the continuous exposure to electron beam. The uses of graphene in this context for static yet hydrated ferritin[9] and bacteria[7,11] have also shown the lowering of radiation damage, possibly by rapid conducting heat and charges. Due to the complicated origins of electron beam damage, the mechanisms for such reduction of electron beam effect have not been thoroughly investigated. In some cases, seemingly controversial observations were reported about the nature of radiation damage, dose dependent or dose rate dependent, and about the state of the liquid environment under electron beam, dried out or truly hydrated. Our observation of a dynamic pyramid in the graphene liquid cell can serve as a good control system for further investigation into the electron beam effect.

We followed the pyramidal artificial molecule used in our 3D remodeling for a prolong time, and found its dramatic structural deformation after 40 seconds of exposure to the electron beam. As highlighted in **Figure 4**, the distance between particles A and B became abruptly large; particle A later diffuses away from the other three component Au nanoparticles. This observation has several indications. The connection between particles A and B was broken once the accumulated electron dose reached a threshold value. And such dose dependent radiation damage is consistent with the previous studies. This dose threshold is larger than that determined from cryogenic TEM imaging of biomolecules[1], but comparable with the reported increased thresholds in both Si_3N_4 and graphene liquid cell experiments[6-8,10-12]. Meanwhile, this transition from a converged 3D pyramidal shape to a dissembled structure proves in return that the pyramidal structure was indeed in liquid and the positions of Au nanoparticles fully described the 3Dconformation of the pyramids.

It is still an open question if the deformed pyramids truly indicate in real time the structural damage of dsDNA in the graphene liquid cell. It is very probable that the breakage of individual bonds in DNA molecules occurs prior to the loss of connecting capability of the DNA chains, therefore prior to the observed phenomenon of Au nanocrystals. Several reasons can lead to this possible gap between the apparent critical dose and the real critical dose for biomolecules. Nanoscale objects have been repeatedly found to have slowed motions[18,21] within the liquid cell configuration. This sluggish motion may effectively act like a “cage” that keeps the structure

altogether from diffusing apart even after the linkage is broken. For the imaging of artificial molecules, this mechanism is efficient enough, as we shown earlier in the text, for us to remodel their 3D conformation.

Of course our use of visual markers, the Au nanoparticles, makes the probing of DNA molecules indirect. A more vigorous and quantitative experiment will be the direct visualization of high-contrast biomolecules, quantify and capture the critical dose that the structural details of biomolecules start to blur or to degrade. Both high-contrast biomolecules, ribosomes for example, and heavy metal ions stained biomolecules can be good candidate systems to show if there is a quantitative improvement of using graphene liquid cell on the tolerance of dosage for biomolecules.

Interaction with the liquid medium

One unique aspect inherent to all liquid cell EM experiment is that electron beam can also interact with the liquid medium besides with the sample of interest[19]. Previous studies have been focused on possible radiation chemistries, where electron beam can produce reactive species to initiate chemical reactions *in situ*.

We look into another frequently observed phenomenon: the intensity fluctuation of the liquid environment during the liquid cell imaging. As shown in **Figure 5**, artificial trimeric molecules rotate in the series of TEM images, together with a visible background fluctuation. One can see clearly the distinct lighter and darker islands in the surrounding liquid environment, with the lighter domains highlighted by red shadows in the TEM images. The positions of the red domains relative to that of trimers randomize from frame to frame, which exhibits little correlation with the motion of trimers. In other words, the motions of trimers are independent from the dynamic fluctuation of liquid environment, which indicates a lower possibility for background fluctuation to be of a convection nature. This lack of correlation, although with the origin of the fluctuation still not resolved, is important since the motions and consequently the imaged configurations of nanocrystals are then not disturbed by the instantaneous flow pattern of the solution.

Conclusions and Outlook

The development of bio-imaging techniques has been associated with important scientific understandings of structures and functions of living systems, and practical applications such as diagnosis and drug engineering. We discussed and demonstrated the unprecedented advantages brought by the recently developed graphene liquid cell EM as a new method of bio-imaging. Graphene liquid cell allows for a unique combination; it has both the native liquid environment enabled by optical microscopy, and the nanometer resolution enabled by electron microscopy. This combination can potentially answer questions that are previously simply not approachable by other experimental techniques, such as the structures of membrane proteins in action in their working environment, the conformational docking of drugs at target proteins, and eventually the

real nanoscale imaging of biomolecules in function and in motion. In the paper, we used Au nanoparticle-DNA artificial molecules, frequently employed for the detection of biomolecular environment, as model systems to illustrate how we can work with the challenges in bio-imaging with graphene liquid cell. We were able to generate 3D shapes of a certain artificial molecule by following its series of 2D projection from continuous rotations. Note that previously people have to either rely on the monodispersity of millions of biomolecules (cryo EM) or on the bulk crystalline form of biomolecule crystals (x-ray crystallography) to do 3D reconstruction. In addition, we show how the small "staining" agents we used to make the invisible biomolecules visible are clearly imaged under graphene liquid cell EM, a unique capability of holding liquid samples in between two ultrathin graphene layers rather than other thicker microfabricated chips. Furthermore, based upon these two capabilities, we followed the structural damage of artificial molecules under the imaging electron beam, and found the structural backbone of artificial molecules was kept stable under a higher electron dose than the previously determined threshold. Although the stability of the artificial molecules can be different from the stability of their biomolecular linkers, more studies from other groups also shown graphene wraps can protect samples under electron beam for both dry and aqueous samples. This protection mechanism, if full quantified and understood, can have huge impact beyond graphene liquid cell EM technique itself. For example, the conventional cryo EM can potentially use graphene wraps to make samples more stable and have better contrast under the imaging beam.

Acknowledgements

This research was supported in part by the Defense Threat Reduction Agency (DTRA) under award HDTRA1-13-1-0035, which provided for in situ TEM experiments, as well as DNA-Au nanoparticle sample preparation; by the National Science Foundation within the Center of Integrated Nanomechanical Systems, under Grant EEC-0832819, which provided for early development of graphene lamination methods. Q.C. was supported by a Miller fellowship from Miller Institute for Basic Research in Science at UC Berkeley. J.S. was supported by Agilent Technologies Applications and Core Technology University Research Grant.

References

[1]Department of Chemistry, [4]Department of Physics, [3]Miller Institute for Basic Research in Science, University of California, Berkeley, CA 94720, United States.

[2]Materials Sciences Division, Lawrence Berkeley National Laboratory, Berkeley, CA 94720, United States.

1. L. F. Kourkoutis, J. M. Plitzko, and W. Baumeister, *Annu. Rev. Mater. Res.* 2012, **42**, 33.

2. J. N. Onuchic, and P. G. Wolynes, *Curr. Opin. Struct. Biol.* 2004, **14**, 70.

3. A. Pulk, and J. H. D. Cate, *Science* 2013, **340**, 1235970.

4. J. W. Miao, H. N. Chapman, J. Kirz, D. Sayre, and K. O. Hodgson, *Annu. Rev. Biophys. Biomol. Struct.* 2004, **33**, 157.

5. K. Xu, G. Zhong, and X. Zhuang, *Science* 2013, **339**, 452.

6. U. M. Mirsaidov, H. Zheng, C. Yosune, and P. Matsudaira, *Biophys. J.* 2012, **102**, L15.

7. F. Banhart, *ChemPhysChem* 2011, **12**, 1637.

8. M. T. Proetto, et al. *J. Am. Chem. Soc.* 2014, **136**, 1162.

9. C. Wang, Q. Qiao, T. Shokuhfar, and R. F. Klie, *Adv. Mater.* 2014, **26**, 3410.

10. D. B. Peckys, and N. de Jonge, *Nano Lett.* 2011, **11**, 1733.

11. N. Mohanty, M. Fahrenholtz, A. Nagaraja, D. Boyle, and V. Berry, *Nano Lett.* 2011, **11**, 1270.

12. S. M. Hoppe, D. Y. Sasaki, A. N. Kinghorn, and K. Hattar, *Langmuir*, 2013, **29**, 9958.

13. Q. Chen, J. M. Smith, J. Park, K. Kim, D. Ho, H. I. Rasool, A. Zettl, and A. P. Alivisatos, *Nano Lett.* 2013, **13**, 4556.

14. S. van de Linde, M. Heilemann, and M. Sauer, *Annu. Rev. Phys. Chem.* 2012, **63**, 519.

15. T. J. Gould, S. T. Hess, and J. Bewersdorf, *Annu. Rev. Biomed. Eng.* 2012, **14**, 231.

16. J. M. Yuk, et al. *Science* 2012, **336**, 61.

17. N. de Jonge, F. M. Ross, *Nat. Nanotechnol.* 2011, **6**, 695.

18. J. Lu, Z. Aabdin, N. D. Loh, D. Bhattacharya, and M. Utkur, *Nano Lett.* 2014, **14**, 2111.

19. J. M. Grogan, N. M. Schneider, F. M. Ross, and H. H. Bau, *Nano Lett.* 2014, **14**, 359.

20. H.-G. Liao, L. Cui, S. Whitelam, and H. Zheng, *Science* 2012, **336**, 1011.

21. H. Zheng, S. A. Claridge, A. M. Minor, A. P. Alivisatos, and U. Dahmen, *Nano Lett.* 2009, **9**, 2460.

22. R. Zan, Q. M. Ramasse, R. Jalil, T. Georgiou, U. Bangert, and K. S. Novoselov, *ACS Nano* 2013, **7**, 10167.

23. G. Algara-Siller, S. Kurasch, M. Sedighi, O. Lehtinen, and U. Kaiser, *Appl. Phys. Lett.* 2013, **103**, 203107.

24. S. E. Lee, A. P. Alivisatos, M. J. Bissell, *Systems Biomedicine* 2013, **1**, 1.

25. A. J. Mastroianni, S. A. Claridge, and A. P. Alivisatos. *J. Am. Chem. Soc.* 2009, **131**, 8455.

26. A. J. Mastroianni, D. A. Sivak, P. L. Geissler, and A. P. Alivisatos, *Biophys. J.* 2009, **97**, 1408.

Figures

Figure1

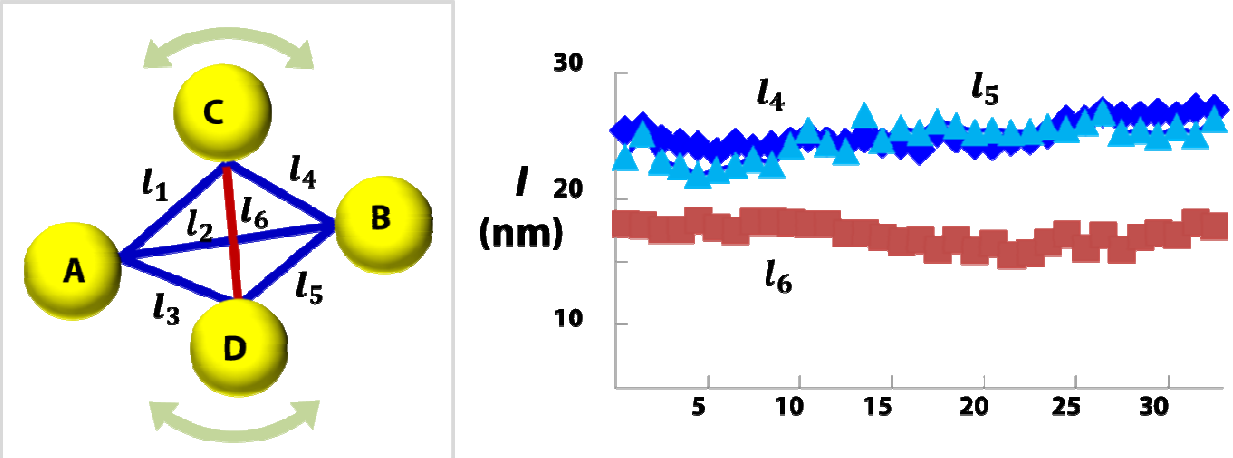

Figure 1: 3D remodeling of artificial pyramidal molecules. **Left**: the designed pyramidal molecule, with the red bond shorter than the other five blue bonds. **Right**: the calculated bond lengths for all the different frames (x axis).

Figure 2

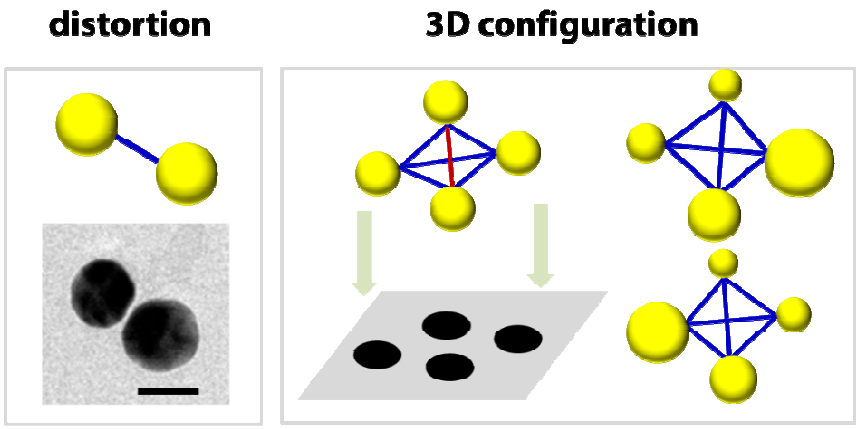

Figure 2: Limitations of dry TEM imaging for artificial molecules. Left: the collapse of a dimeric artificial molecule. Right: the flattening of a pyramidal artificial molecule. Scale bar: 20 nm.

Figure 3

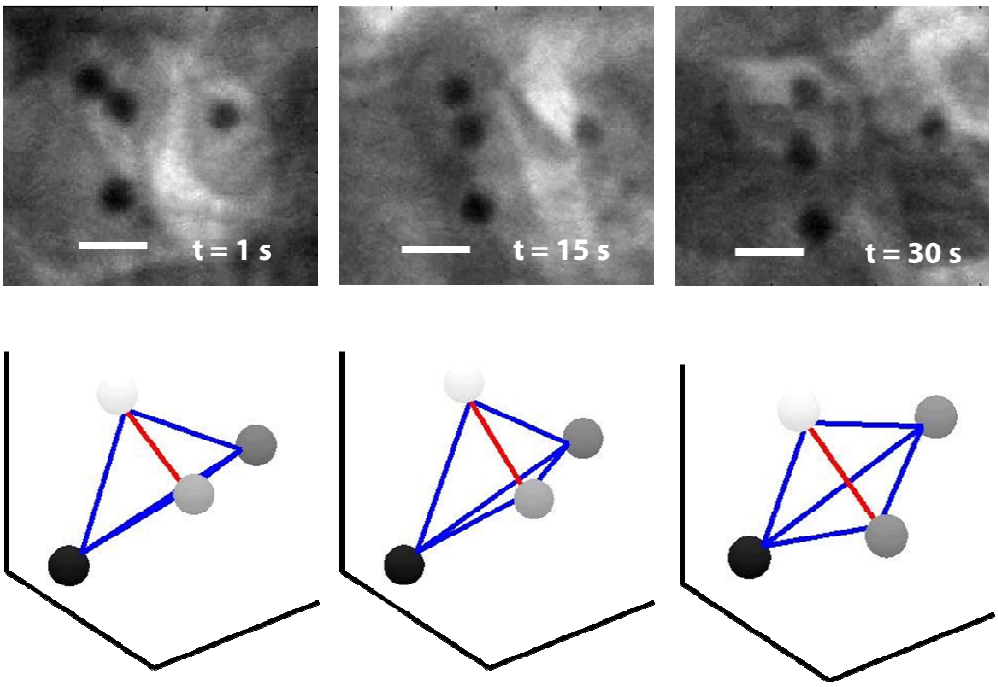

Figure 3: Snapshots of a continuous TEM movie (top) and the corresponding 3D models (bottom). Scale bars are 10 nm. The spheres in the 3D models are color coded according to their z height.

Figure 4

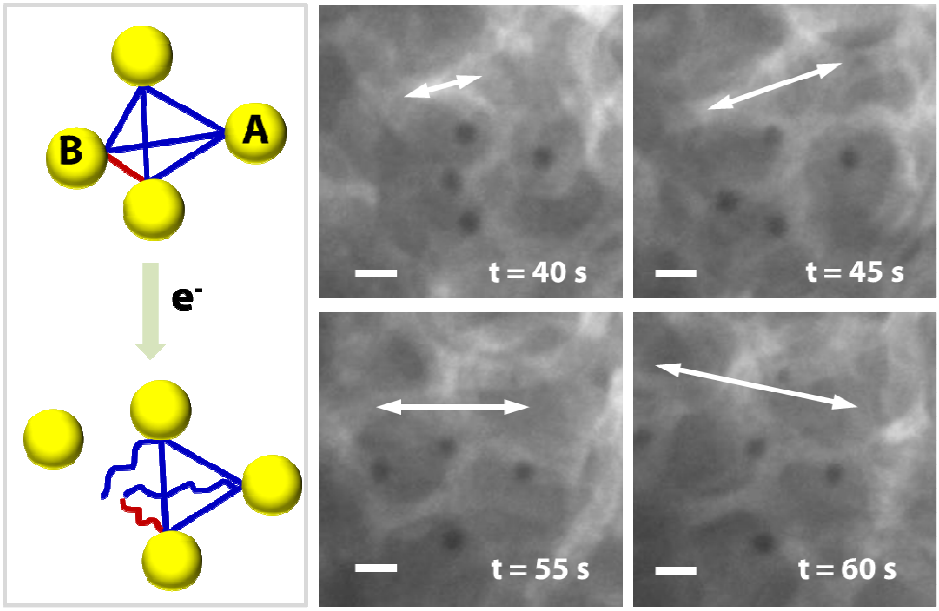

Figure 4: The breakage of DNA linkage after imaging the pyramid shown in Figures 2 and 3 for a longer time. Left: schematics. Right: TEM series, where the arrows highlighted the distance between particles A and B. Scale bar is 10 nm.

Figure 5

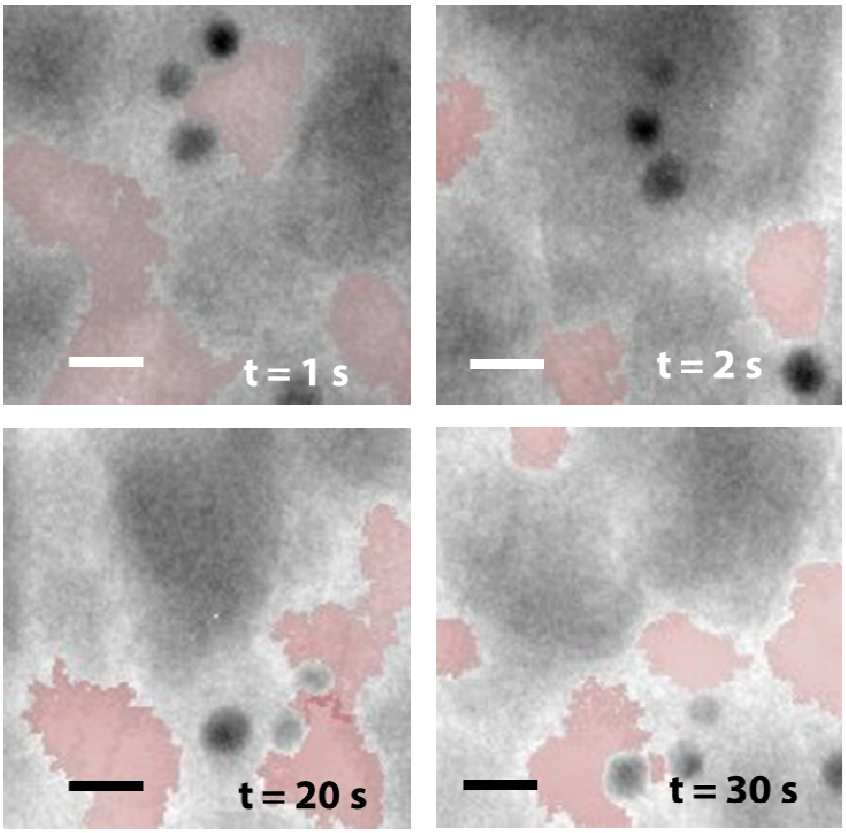

Figure 5: Snapshots of a continuous TEM movie of a trimeric artificial molecule. Red shadows highlight areas of high intensity. Scale bar: 6 nm